ELSEVIER

Journal of Power Sources 81–82 (1999) 200–206

JOURNAL OF POWER SOURCES

www.elsevier.com/locate/jpowsour

Early studies on anodic properties of lithium intercalated graphite

Samar Basu *

Bell Laboratories, Lucent Technologies, Holmdel, NJ 07733, USA

Abstract

Early electrochemical studies on lithium intercalated graphite, LiC_6, which were conducted to establish the anodic properties of these materials in rechargeable lithium cells are reported. Two types of electrochemical cells, a group of cells at high temperature and another group at ambient temperature, were utilized in these studies. The electrode potential of LiC_6 against a pure lithium reference electrode was in the range of 30–35 mV. The cell voltage of $LiC_6/Li^+/NbSe_3$ cells at ambient temperature was 2.770 V. The cycling characteristics and reversibility of the LiC_6 electrode were also excellent. These studies established that lithium intercalated graphite is capable of performing well as an anode in rechargeable lithium cells replacing pure elemental lithium with a negligible loss of cell voltage. Photoemission studies conducted earlier on LiC_6 indicated that lithium exists predominantly as lithium ions in this material which helps to avoid the formation of highly reactive elemental lithium at the anode/electrolyte interface during the recharging process.
© 1999 Elsevier Science S.A. All rights reserved.

Keywords: Lithium intercalated graphite; Anode; Electrochemical

1. Introduction

The development and commercialization of rechargeable lithium batteries have received considerable attention in the past two to three decades. A major reason for this is the proliferation of portable communication devices (e.g., cellular phones, cordless phones, personal digital assistants, etc.), laptop computers, video cameras, and VCRs, all of which have a critical dependence on the availability of high energy density rechargeable power sources.

Ambient temperature rechargeable lithium batteries have received most attention due to the low specific weight of the metal. In these lithium cells, organic solvents with dissolved lithium salts were quickly identified as the electrolyte of choice. A large number of cathode materials such as $NbSe_3$, V_6O_{13}, TiS_2, MnO_2, TaS_2, FeS_2, etc., were identified, developed, and patented in the last two or three decades. These cathodes are capable of supporting a large number of charge/discharge cycles at significant current densities without serious degradation of structural and electrochemical properties.

On the other hand, the lithium anode in these non-aqueous cells has provided a formidable technological challenge. In non-aqueous cells, the lithium anode suffers from side reactions with the organic electrolyte during cycling. The high reactivity of lithium metal is presumably the primary reason for the side reactions between the freshly formed elemental lithium and the organic electrolyte at the anode–electrolyte interface during cell recharging. These side reactions lead to the formation of films on the anode surface and a corresponding loss of lithium metal. Over a large number of charge/discharge cycles, the cumulative loss of metallic lithium can be significant. For a practical device, the anode:cathode ratio has to be in the range of 5–10, instead of the ideal stoichiometric ratio of 1:1. The excess lithium in such a device leads to a reduction in energy density of the cell, sacrificing the primary advantage of lithium cells.

Another problem associated with the lithium anode in a practical battery system is the fire hazard represented by elemental lithium. The relatively low melting point of the metal carries the risk of generating a pool of molten lithium due to accidental overheating.

The combination of these problems led the scientific community to investigate alternate vehicles for lithium in rechargeable lithium cells. Alloys of lithium, such as the lithium–aluminum alloy, were explored as alternatives. However, the electrode properties of the alloys at ambient temperature were not encouraging.

Graphite Intercalation Compounds (GICs) are a group of novel materials which originally were studied primarily

* Tel.: +1-732-949-1040; Fax: +1-732-949-1196; E-mail: sbasu@lucent.com

0378-7753/99/$ - see front matter © 1999 Elsevier Science S.A. All rights reserved.
PII: S0378-7753(98)00212-2

by physicists for their interesting structural and physical properties. It was the exceedingly high electrical conductivity and other semi-metallic properties exhibited by this class of materials which attracted the attention of scientists. Intercalation of both electron donors (e.g., alkali metals) and acceptors (e.g., AsF_5) between layers of carbon along the *c*-axis of the hexagonal graphite lattice results in remarkable changes in physical properties. Lithium intercalated graphite, especially the stage I compound, LiC_6, was considered a model material among the alkali metal GICs due to its simple electronic structure. There were many theoretical predictions [1,2] regarding the structure and electronic properties of lithium GICs. However, experimental work could not be carried out due to the difficulties in synthesizing the materials in suitable size, shape, and quantity. Synthesis of the lithium GIC in Highly Oriented Pyrolytic Graphite (HOPG) was considered extremely important in the mid-seventies.

Synthesis of LiC_6 was first reported by Guérard and Hérold [3] in 1975. The vapor phase synthesis technique was cumbersome, and only polycrystalline material could be prepared. The simplified liquid phase synthesis of LiC_6 and LiC_{18} using HOPG developed by us was reported in 1978 [4]. The focus of attention on these materials at that time was on their electrical conductivity, reflectivity, and other physical properties. Results of our studies on the two compounds, stage I LiC_6, and stage II LiC_{18}, were reported [5–8].

High chemical reactivity of the intercalated lithium in these compounds was observed during the preparation and handling of these materials. The high chemical reactivity (i.e., chemical potential) of the intercalated lithium provided an early indication that these materials might be suitable as anodes in rechargeable lithium cells with only a minor loss of cell voltage. The rate of formation of LiC_6 and LiC_{18} during liquid phase intercalation in a molten lithium pool was a strong indication of high diffusivity of lithium in these solid structures. Since chemical potential and diffusivity are the two most important properties of any practical electrode system, these two observations provided early indications that lithium intercalated graphite could be used as an anode in rechargeable lithium cells.

Electrochemical cells were setup to determine and evaluate the anodic properties of these materials in non-aqueous cells at high temperature as well as at ambient temperatures. These early studies demonstrated the feasibility of using lithium intercalated graphite in practical battery systems and led to patents for both the high temperature [9] and ambient temperature [10] systems. These experiments demonstrated the anodic properties of these novel materials which provided the technological foundation and basis for the Lithium Ion Batteries currently being manufactured by various commercial vendors. This paper communicates further results of some of these experiments.

2. Experimental

2.1. Material preparation

2.1.1. LiC_6

Lithium intercalated graphite was prepared by the liquid phase intercalation process described earlier [4,5]. Polycrystalline graphite rods (99.5% pure) and Highly Oriented Pyrolytic Graphite (HOPG, 99.8% purity), both from Union Carbide, were inserted into molten pools of lithium at 350°C inside an argon atmosphere glove box. Intercalation reactions took 3–8 h, depending on the cross-section, to produce the bright shining golden color stage I LiC_6. After the reactions were complete, the graphite rods and HOPG

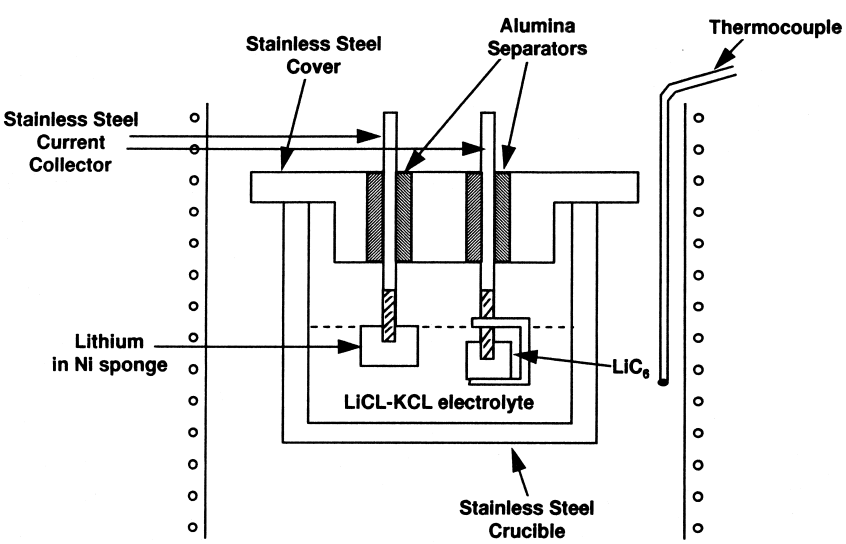

Fig. 1. Schematic diagram of high temperature $Li/Li^+/LiC_6$.

pieces were removed from the molten lithium pools. The samples were cleaned by cleaving and scraping excess metal from the surfaces. For longer term storage, the LiC_6 samples were vacuum-sealed in glass tubes.

2.1.2. Electrolyte

For the experiments at high temperature, a mixture consisting of 58 mol% LiCl and 42 mol% KCl was used. Both of these salts were 99.9% pure. The adsorbed moisture was removed from the salts by vacuum baking at 150°C. For most of the experiments, the molten salt mixtures were pre-equilibrated with molten lithium at 380°C to eliminate traces of moisture and/or OH^- ions.

The ambient temperature experiments were conducted with organic solvents such as 2-methyltetrahydrofuran-(2MeTHF), propylene carbonate, 1,3 dioxolane and tetraglyme. Both pure solvents and binary mixtures were used. Lithium hexafluoroarsenate, $LiAsF_6$, was used as the salt. The performance of $LiAsF_6$ was superior to other lithium salts which was subsequently confirmed by others [11,12].

2.1.3. Cathode

For the ambient temperature experiments, niobium triselenide, $NbSe_3$, was used as the cathode material. The preparation and characterization of this material was reported earlier [13].

2.1.4. Reference electrode

For the high temperature experiments, the lithium reference electrode was prepared by inserting a rectangular piece of nickel sponge in a pool of molten lithium metal inside an argon atmosphere glove box. Excess lithium was scraped from the nickel sponge after withdrawal from the molten lithium pool. The reference electrodes were freshly made just prior to the experiments.

For ambient temperature experiments, lithium rods (9.5 mm diameter) with freshly scraped surfaces were used.

2.2. Cell description

The high temperature cell is shown schematically in Fig. 1. The LiCl–KCl electrolyte mixture was contained in a 38 mm diameter stainless steel (type 304) crucible. Two 3.2 mm diameter stainless steel rods were used as current collectors. A stainless steel lid covered the cell at the top. The current collectors passed through two holes in the lid. Tight-fitting alumina tubes in the lid around the current collectors were used as insulators. It was important to have a tight fit between the crucible and the lid in order to reduce temperature gradients within the electrolyte. A thermocouple was placed next to the stainless steel crucible to measure the cell temperature. The ends of the current collectors were threaded and the lithium reference electrode was screwed onto the current collector. The LiC_6 electrode was pinned down to the current collector assembly by threads as shown in Fig. 1. The entire cell assembly was lowered down into the constant temperature zone of a pot furnace operating inside the argon-filled glove box. The temperature of the cell assembly was maintained at 375°C ± 5°C.

The ambient temperature cell is shown schematically in Fig. 2. The cell casing was machined from a Halar (a trademark of AlliedSignal) rod of 25.4 mm diameter. Two 12.7 mm diameter stainless steel (type 304) screws were used as current collectors. A fiberglass filter paper separator soaked with organic electrolyte was positioned at the center of the cell by applying pressure by tightening the screws from both ends.

Polycrystalline anodes (LiC_6) and cathodes ($NbSe_3$) were pressed into 9.5 mm diameter pellets of thickness between 1.6–4.8 mm. HOPG anodes did not require pressing, and were cleaved to the appropriate thickness. In the ambient temperature experiments, the temperature varied between 23–27°C.

A few ambient temperature experiments for open circuit voltage measurements were carried out in beakers using a

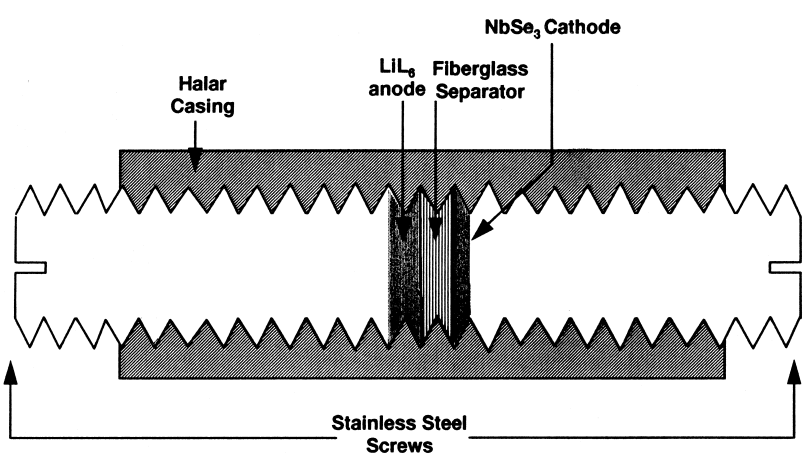

Fig. 2. Schematic diagram of ambient temperature $Li/Li^+/NbSe_3$ cell.

set-up similar to Fig. 1. Pure lithium rods were used as reference electrodes in these experiments.

3. Results and discussion

3.1. High temperature experiments

3.1.1. Cells without pre-equilibration

Initially, the following cell was set up at 375°C:

$$Li/Li^{+}(\text{in LiCl–KCl})/LiC_6(\text{in HOPG})\ldots \quad (1)$$

The open circuit voltage of these cells usually started out at 0.035 V. However, after a few hours of stable voltage, a definite trend of slow increase in cell voltage was observed in all cases. Constant currents through these cells in the range of 2–20 mA were allowed to pass to strip and plate lithium into the LiC_6 electrodes. At the end of each discharge/charge cycle, the equilibrium cell voltages in these cells showed a constant increase in value. The lack of reproducible equilibrium cell voltage at the end of each discharge/charge cycle strongly indicated contamination of the cell components and/or presence of side reactions in these cells. At the end of cycling, the LiC_6 electrodes were withdrawn from these cells, cooled to room temperature, and then the electrodes were cleaved. The electrodes showed the steel blue color, typical [5] of stage II LiC_{18}. This strongly indicated that the starting material (i.e., LiC_6) was not being regenerated at the end of discharge/charge cycles in these experiments. The dissolution of lithium either from the reference electrode and/or from LiC_6 was suspected in these experiments.

A known amount of the LiCl–KCl electrolyte from one of these cells was dissolved in distilled water and titrated with 0.1 normal hydrochloric acid. The solution was alkaline, and the concentration of dissolved metallic lithium in the electrolyte was estimated to be 3.3×10^{-4} g per g of electrolyte.

3.1.2. Pre-equilibrated cells

All subsequent experiments were carried out using LiCl–KCl electrolyte pre-equilibrated with molten lithium at 380°C for 12 h before insertion of LiC_6 and reference electrodes. A stable open circuit voltage of 0.035 V was observed in these cells even after several discharge/charge cycles. A high activity of lithium in LiC_6 is demonstrated by the low equilibrium cell voltage. The negligible loss of only 0.035 V in the overall cell voltage is very attractive from the standpoint of practical battery systems.

Fig. 3 shows the dynamic cell voltage of an HOPG LiC_6 electrode at 375°C in a $Li/Li^{+}/LiC_6$ cell. At the beginning of the first deintercalation of lithium from the electrode, the cell voltage typically increases to a higher value (the hump in Fig. 3) before settling down to a lower plateau. This phenomenon was observed in all the experiments. The hump could be due to a number of factors, such as surface contamination at the LiC_6–electrolyte interface, presence of impurities in the LiC_6 lattice hindering diffusion of lithium in LiC_6, etc. It is interesting to note

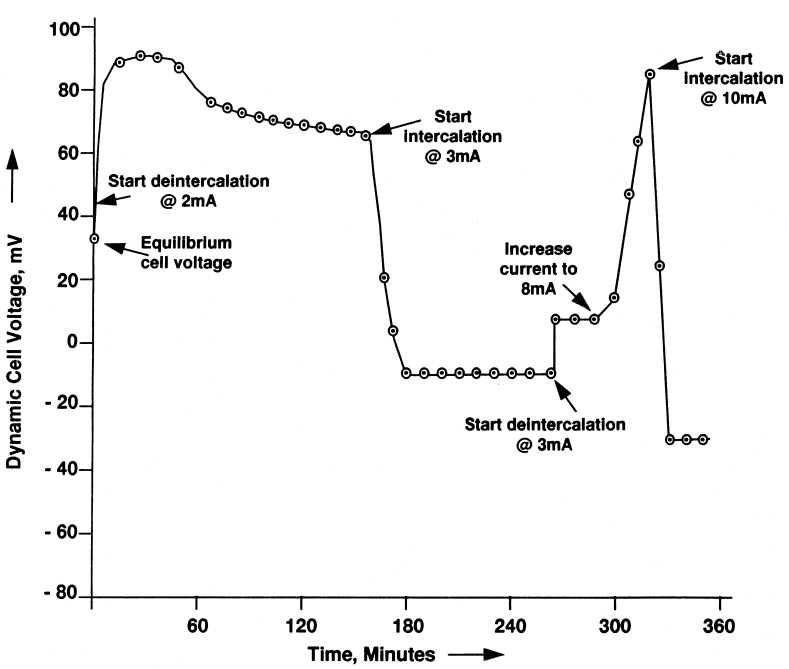

Fig. 3. Initial cycling of $Li/Li^{+}/LiC_6$ cells with time.

that the hump effect was not observed after the first cycle. Fig. 4 shows the cycling characteristics of an LiC_6 electrode, after the initial effects represented by the first few cycles are over.

In each discharge/charge cycle (i.e., deintercalation–intercalation step), exactly same amount of charge was allowed to flow in each direction, such that at the end of each cycle, the starting composition of the lithium intercalated graphite was always regenerated. In Fig. 4, the plateau region at the start of each deintercalation step reflects the constant chemical potential of lithium in a two phase mixture of stage I (LiC_6) and stage II (LiC_{18}) compounds. It is clear that after the disappearance of the voltage hump in the first cycle (Fig. 3), the voltage plateaus in the subsequent cycles become flatter. The LiC_6 electrode behaves more like an 'ideal electrode' after the first few cycles as shown in Fig. 4. A constant charge of 54 C was passed through the cell in Fig. 4 to intercalate and deintercalate lithium in graphite by passing a constant current of 20 mA. The theoretical capacity of the LiC_6 electrode in Fig. 4 based on its lithium content was 61.1 C. The sharp spike in voltage at the ends of voltage plateaus in deintercalation is indicative of depletion of the mixture of stage I and stage II compounds in the graphite lattice, and the predominance of the single phase stage II LiC_{18} compound.

After the termination of the cell shown in Fig. 4, the HOPG electrode was cleaved after cooling to room temperature. The bright golden color of stage I LiC_6 was observed, which indicated that the starting material was regenerated at the end of cycling in the cell.

3.2. Ambient temperature experiments

3.2.1. Cells without pre-equilibration

Initially, the following cells were set up at ambient temperature inside a beaker in an arrangement similar to Fig. 1:

$$Li/Li^+(LiAsF_6 \text{ in organic solvents})/LiC_6(\text{in HOPG})\ldots \quad (2)$$

The equilibrium cell voltage was 0.030 ± 0.002 V. The LiC_6 electrode was observed to be extremely sensitive to contaminants in the electrolyte. In the first few cells, the bright golden color of the stage I lithium intercalated graphite was observed to tarnish in a few hours after insertion into the electrolyte and the cell voltage showed a slow but constant increase over a long period of time. The increase in cell voltage was remarkably similar to that observed in the high temperature experiments without pre-equilibration. Hence, in subsequent cells, the electrolyte was pre-equilibrated with LiC_6 for a few days at ambient temperature, and then new cells were set up using the pre-equilibrated electrolyte.

3.2.2. Pre-equilibrated cells

The bright golden color of LiC_6 did not change in these cells, and the equilibrium cell voltage was stable over a long period of time. The equilibrium cell voltage was within the range of 0.028–0.032 V. This compares well with the 0.035 V observed in the high temperature cells. Comparison of the equilibrium cell potential data between the high temperature and ambient temperature cells indi-

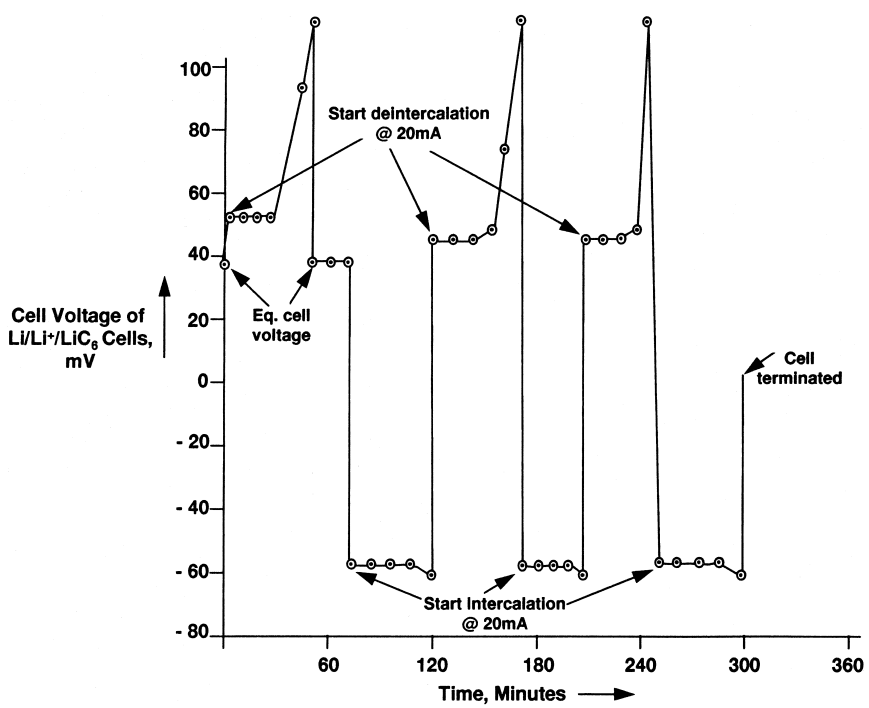

Fig. 4. Cycling characteristics of $Li/Li^+/LiC_6$ cells after first few cycles.

cates that the electrode potential of lithium intercalated graphite does not have a strong temperature dependence; which is a highly desirable property for any electrode system. The electrode potentials of the ambient temperature cells were quite reproducible after stripping and plating of lithium from the LiC_6 electrode by passing constant currents of 0.1–1.5 mA through the cells. Since these cells were set up to determine the equilibrium cell voltage and reversibility of the LiC_6 electrode, and not optimally designed to reduce internal impedance, current levels higher than 1.5 mA were not attempted.

Fig. 5 shows the change in dynamic cell voltage with time in the first few deintercalation and intercalation steps during cycling of a cell described by Eq. (2). The voltage hump observed in the high temperature cells (see Fig. 3) was also observed in these ambient temperature cells. As mentioned earlier, during each discharge/charge (i.e., deintercalation–intercalation steps) cycle, exactly same amount of charge was passed through the cells to regenerate the initial composition of the LiC_6 electrode at the end of each cycle.

A few cells using $NbSe_3$ cathodes (see Fig. 2) were set up at ambient temperature:

$$LiC_6/Li^+(LiAsF_6 \text{ in organic electrolyte})/NbSe_3 \ldots \quad (3a)$$

The equilibrium cell voltage was 2.770 V. Since the electrode potential of LiC_6 electrode against the lithium reference electrode is 0.030 V, this is in excellent agreement with the voltage of 2.800 V in $Li/Li^+/NbSe_3$ cells reported earlier [13]. The cycling characteristics of this cell at a discharge current of 1.0 mA and a charge current of 0.1 mA are shown in Fig. 6. The cell was terminated after 20 cycles, when an internal short circuit was suspected.

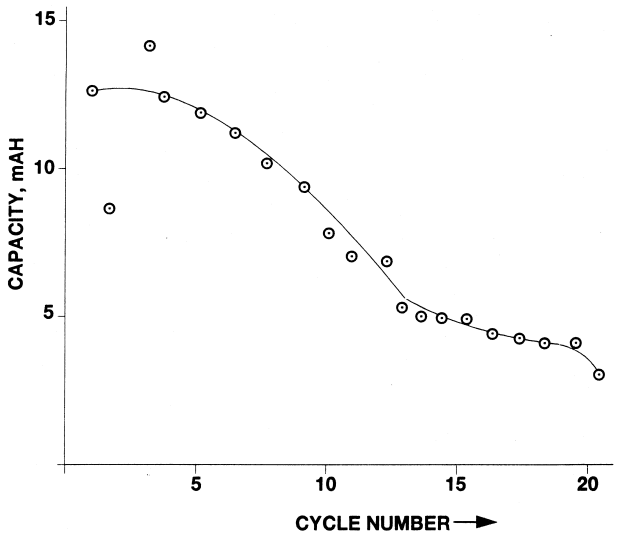

Fig. 6. Cycling characteristics of an $NbSe_3$ cell with LiC_6 anode at ambient temperature.

The reversibility of the lithium intercalated graphite electrode is indicated by the data in these experiments. It is important to note that the cells in these experiments were not designed to reduce internal cell impedance and maximize discharge/charge currents. With proper design of cells, in a practical battery system, these parameters may be optimized.

During the recharge cycle in a lithium cell, the following reaction is expected to take place at the lithium–electrolyte interface:

$$Li^+ + e = Li^0 \ldots \ldots \quad (3b)$$

where Li^+ represents a lithium ion in the electrolyte and Li^0 represents a freshly neutralized lithium atom on the

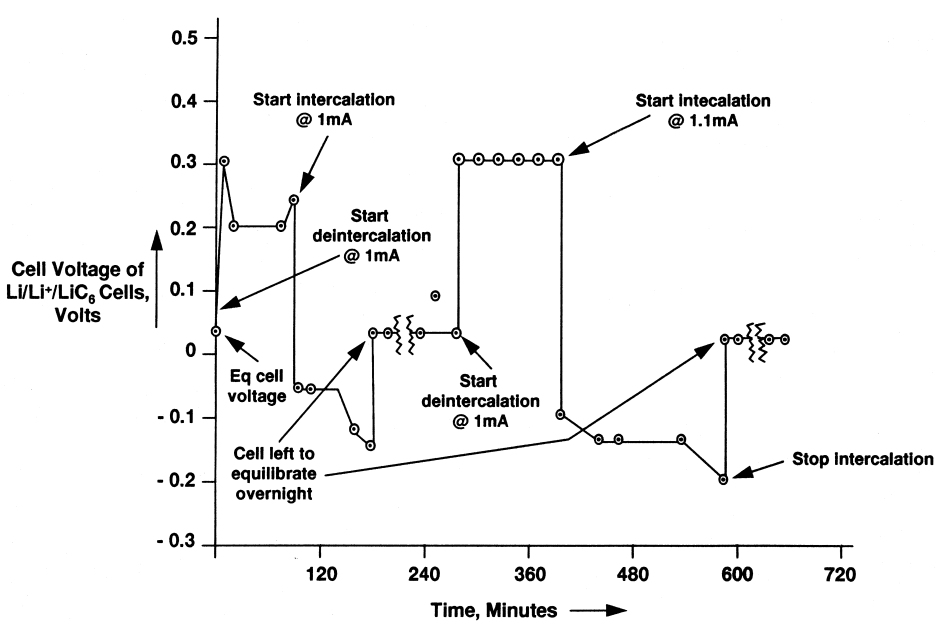

Fig. 5. Dynamic cell voltage in $Li/Li^+/LiC_6$ (HOPG) cells.

surface of the anode. This highly reactive lithium is most likely to react with the organic electrolyte producing a thin film on the anode surface [14,15].

Photoemission studies reported earlier [6–8] by us on lithium intercalated graphite, indicated that lithium predominantly exists as Li^+ ion in these materials. As a result, most of the lithium ions arriving at the anode/electrolyte interface during cell recharging will not have to go through the stage of formation of highly reactive lithium atoms depicted by Eq. (3b), which leads to the film formation on the anode surface. Hence, this ionic nature of intercalated lithium in LiC_6 provides the primary underpinning for the success of lithium intercalated graphite as an anode in a lithium cell during the recharging of a discharged cell.

An additional advantage provided by the LiC_6 anode in a practical battery system is that the fire hazard represented by elemental lithium metal in a battery is reduced significantly by the use of a lithium intercalated graphite anode.

3.2.3. Future direction

In the future, fundamental studies on this material will be necessary to fully understand the performance of this electrode in lithium cells. Measurements of diffusion coefficient and the mechanism of diffusion of Li^+ in the LiC_6 lattice are important areas of future work. The influence of traces of other intercalants, the influence of morphology of graphite [16] and its change, the source of graphitic material, etc., are critical areas of research for the advancement of this technology. In this regard, the US Government sponsored initiative under the auspices of the Department of Energy at Sandia National Laboratory to create a Cooperative Research and Development Agreement based on US Patents 4,304,825 [9] and 4,423,125 [10] to explore and advance this technology is quite commendable.

Although the fire hazard represented by elemental lithium has been reduced by lithium intercalated graphite, still fire safety will continue to be an important issue for this technology. Advances in microprocessor and microcontroller technologies offer interesting capabilities in controlling currents through individual cells in practical battery systems these days. It is hoped that these semiconductor devices will be able to make lithium batteries safer than they are today.

4. Summary

Early electrochemical studies on lithium intercalated graphite established the anodic properties of the material in rechargeable lithium cells at ambient temperature as well as at elevated temperature (375°C). The reversibility of the electrode was excellent, and the loss of cell voltage was negligible ($\sim$ 30–35 mV). The performance of the electrode is explained by the predominant existence of lithium as lithium ions in the lattice, which was demonstrated by the photoemission studies on these materials. The formation of highly reactive lithium atoms on the surface of the anode is eliminated during recharging due to the ionic existence of lithium in these materials.

References

[1] N.A.W. Holzworth, S. Rabii, Mater. Sci. Eng. 31 (1975) 195.
[2] N.A.W. Holzworth, S. Rabii, L.A. Girifalco, Phys. Rev., Sec. B 18 (1978) 5190.
[3] D. Guérard, A. Hérold, Carbon 13 (1975) 337.
[4] M. Zanini, S. Basu, J.E. Fischer, Carbon 16 (1978) 211.
[5] S. Basu, C. Zeller, P. Flanders, C.D. Fuerst, W.D. Johnson, J.E. Fischer, Mater. Sci. Eng. 38 (1979) 275.
[6] G.K. Wertheim, P.M.Th.M. Van Attekum, S. Basu, Solid State Commun. 33 (1980) 1127.
[7] S.B. Dicenzo, S. Basu, G.K. Wertheim, Synthetic Metals 3 (1981) 139.
[8] S. Basu, G.K. Wertheim, S.B. Dicenzo, Lithium: current applications in science, medicine and technology, in: R.O. Bach (Ed.), Chap. 13, Wiley, New York, 1985.
[9] S. Basu, U.S. Patent No. 4,304,825, Dec. 8, 1981.
[10] S. Basu, U.S. Patent No. 4,423,125, Dec. 27, 1983.
[11] D. Aurbach, Y. Ein-Eli, B. Markovsky, A. Zaban, S. Luski, Y. Carmeli, H. Yamin, J. Electrochem. Soc. 142 (1995) 2882.
[12] E.J. Plichta, W.K. Behl, J. Electrochem. Soc. 140 (1993) 46.
[13] S. Basu, F.A. Trumbore, J. Electrochem. Soc. 139 (1992) 3379.
[14] D. Aurbach, M.L. Daroux, P.W. Faguy, E. Yeager, J. Electrochem. Soc. 134 (1987) 1611.
[15] I. Yoshimatsu, T. Hirai, J. Yamaki, J. Electrochem. Soc. 135 (1988) 2422.
[16] M.W. Verbrugge, B.J. Koch, J. Electrochem. Soc. 143 (1996) 27.